

Top Quark Seesaw Theory of Electroweak Symmetry Breaking

R. Sekhar Chivukula¹, Bogdan A. Dobrescu²,
Howard Georgi³, Christopher T. Hill^{2,4}

¹*Physics Department, Boston University
Boston, Massachusetts 02215, USA **

²*Fermi National Accelerator Laboratory
P.O. Box 500, Batavia, Illinois 60510, USA †*

³*Harvard University
Cambridge, Massachusetts 02138, USA ‡*

⁴*The University of Chicago
Chicago, Illinois 60637, USA*

Abstract

We study electroweak symmetry breaking involving the seesaw mechanism of quark condensation. These models produce a composite Higgs boson involving the left-handed top quark, yet the top mass arises naturally at the observed scale. We describe a schematic model which illustrates the general dynamical ideas. We also consider a generic low-energy effective theory which includes several composite scalars, and we use the effective potential formalism to compute their spectrum. We develop a more detailed model in which certain features of the schematic model are replaced by additional dynamics.

*e-mail address: sekhar@bu.edu

†e-mail addresses: bdob@fnal.gov, hill@fnal.gov

‡e-mail address: georgi@physics.harvard.edu

1 Introduction

The Higgs doublet of the standard model, used to break the electroweak symmetry and generate all observed quark, lepton and gauge boson masses, does not have to be a fundamental field. In fact, the fermions observed so far have the appropriate quantum numbers to provide the constituents of a composite Higgs field. Therefore, it is interesting to consider the existence of some new, non-confining strong interactions which bind the quarks and/or leptons within a composite Higgs field, giving rise to a condensate (associated with a Higgs VEV) and to Higgs-Yukawa couplings.

Due to its large mass, the top quark is a natural candidate for providing a constituent to a composite Higgs boson and an electroweak symmetry breaking (EWSB) condensate [1, 2]. However, the computation of the W and Z masses to leading order in $1/N_c$ (N_c is the number of colors) shows that the quark whose condensate gives the bulk of EWSB must have a mass of order 0.6 TeV (in the absence of an excessively fine-tuned version of the model in which the new strong dynamics is placed at the GUT scale). Such a heavy quark may, in principle, be part of a fourth generation, but in that case one would have to worry about the proliferation of weak-doublet fermions that contribute to the electroweak radiative parameter S , and the top would not be directly involved in the EWSB mechanism.

In a previous letter [3] two of us introduced the idea of a dynamical top quark seesaw mechanism. Here the EWSB occurs via the condensation of the left-handed top quark, t_L , with a new, right-handed weak-singlet quark, which we refer to as a χ -quark. The χ_R quark has hypercharge $Y = 4/3$ and thus is indistinguishable from the right-handed top, t_R . The dynamics which leads to this condensate is essentially topcolor [4, 5]. The fermionic mass scale of this weak-isospin $I = 1/2$ condensate is large, of order 0.6 TeV. This corresponds to the formation of a dynamical boundstate weak-doublet Higgs field, $\sim (\overline{\chi_R}t_L, \overline{\chi_R}b_L)$. To leading order in $1/N_c$ this yields a VEV for the Higgs boson of the appropriate electroweak scale, $v/\sqrt{2} \approx 175$ GeV. However, the model also incorporates a new left-handed weak-singlet χ -quark, with $Y = 4/3$. The χ -quarks condense amongst themselves through additional new dynamics at still larger mass scales. Moreover, the left-handed χ -quark has a weak-singlet condensate with the right-handed top quark. There is *ab initio* no direct left-handed top condensate with the right-handed anti-top in this scheme (or else this condensate is highly suppressed).

Upon diagonalization of the fermionic mass matrix this admits a conventional seesaw

mechanism, yielding the physical top quark mass as an eigenvalue that is less than the 600 GeV matrix element. Thus, the top quark mass can be adjusted naturally to its experimental value. The diagonalization of the fermionic mass matrix in no way affects the fact that the model has a composite Higgs doublet, with a VEV of $v/\sqrt{2} \approx 175$ GeV. The mechanism incorporates t_L , which provides the source of the weak $I = 1/2$ quantum number of the composite Higgs boson, and thus the origin of the EWSB vacuum condensate. Topcolor and any additional strong dynamics is occurring at a multi-TeV scale, and the observed top quark mass arises naturally, being suppressed by a ratio of \sim TeV scales. Indeed, if a mechanism like this operates in nature, then we have already observed the key $I = 1/2$ element of EWSB at the Tevatron !

There are several attractive features of this mechanism. First, while there are the additional χ quarks involved in the strong dynamics, *these do not carry weak-isospin quantum numbers*. This is a remarkable advantage from the point of view of model building. The counting constraints of technicolor, e.g., on the number of techniquarks from the S parameter, are essentially irrelevant for us, since we have only a top quark condensate in the EWSB channels. The constraints on custodial symmetry violation, i.e., the value of the $\Delta\rho$ or equivalently, T parameter, are easily satisfied, being principally the usual m_t contribution, plus corrections suppressed by the seesaw mechanism [3].

Second, the models make a robust prediction about the nature of the electroweak condensate: the left-handed top quark is unambiguously identified as the electroweak-gauged condensate fermion. The scheme demands the presence of some kind of topcolor interactions, new strong interactions associated with the formation of the top condensate. This implies that QCD itself will change character at the multi-TeV scale as it is embedded into the larger topcolor containing gauge group. However, beyond the $I = 1/2$ component of the EWSB, the remainder of the structure, e.g., the χ -quarks and the additional strong forces which they feel, is somewhat arbitrary at this point.

Third, the scheme implies that in the absence of the seesaw, the top quark would have a larger mass, of order 600 GeV. This in turn leads to a relaxation of the constraints on the masses of topcolor colorons and any additional heavy gauge bosons, permitting the full topcolor structure to be moved to somewhat higher mass scales. This gives more model-building elbow room, and may reflect the reality of new strong dynamics.

We believe the top quark seesaw is a significant new idea in dynamical models of EWSB and opens up a large range of new model building possibilities. For that reason we will give a fairly detailed discussion of the seesaw mechanism in this paper.

We begin in Section 2 with the presentation of a schematic model. Here the electroweak condensate involving \overline{t}_L and χ_R is driven by topcolor interactions, but the weak-singlet condensates involving $\chi_{L,R}$ and t_R are simply mass terms that we implement by hand. This naturally separates the problem of EWSB from the weak-singlet physics in the $\chi_{L,R}$ and t_R sector, which is the key advantage of the seesaw mechanism. We derive the effective Lagrangian for the dynamical Higgs and its interactions with matter using the renormalization group approach in the large- N_c fermion-bubble approximation. The schematic model shows the emergence of the Higgs boundstate and the formation of the $\overline{\chi}_R t_L$ condensate. The schematic model provides a point of departure for the construction of more elaborate models, and the problem of generating light fermion Higgs-Yukawa couplings, which we will not address in detail. We will briefly summarize options for addressing the problem of the b -quark mass in the schematic model. The Higgs boson mass is large in the schematic model, given by $2m_{t\chi} \sim \mathcal{O}(1 \text{ TeV})$ in the large- N_c fermion-bubble approximation, essentially saturating the unitarity bound of the standard model [6].

In Section 3 we proceed with a more ambitious attempt to include additional interactions amongst the minimal set of fermions of the schematic model. This is a somewhat general construction, and it leads to additional composite scalars, and new effects. We give a full effective potential analysis of this scheme. Weak-singlet mass terms are still required as in the schematic model to trigger the desired tilting of the vacuum, though they can now be much smaller than in the schematic model since the additional strong, yet subcritical, interactions can amplify the effects of these mass terms [7]. These interactions push the potential close to a second order (or weakly first-order) phase transition and thus, the Higgs boson can be as light as $\sim 100 \text{ GeV}$. This requires a partial degeneracy between the weak-doublet and weak-singlet composite scalars. In the decoupling limit the more general theory resembles the standard model with a light Higgs boson.

In Section 4, we describe a class of models incorporating the top quark seesaw mechanism in which topcolor symmetry breaking is dynamically generated. These models can replace the explicit weak-singlet mass terms with additional dynamics, in analogy to extended technicolor. These models also allow in principle for the generation of masses of the light quarks and accommodate intergenerational mixing. While these models do not yet provide a complete explanation of flavor symmetry breaking, we regard them as an existence proof and a guide to future theoretical investigations.

Section 5 summarizes our conclusions. In Appendix A we apply the effective potential

formalism of Section 3 to the top quark seesaw model of ref. [3]. In Appendix B we prove that the coupled gap equations used in ref. [3] are equivalent with the stationarity conditions of the effective potential derived in Section 3.

2 A Schematic Model

In the present Section we will study a schematic model of the top quark seesaw. This model will be a minimal version of the top seesaw and is intended primarily to exhibit the essential physics. The schematic model contains the elements of the third generation, the left-handed top-bottom doublet, $\psi_L = (t_L, b_L)$, the right-handed top quark, t_R , (we will postpone discussing the right-handed b -quark and associated fields for the moment; indeed, the present model will not be anomaly free without the inclusion of b_R and associated fields, so we return to consider it below). We further introduce two weak-singlet fermions, χ_R and χ_L , each having the quantum numbers of t_R . The schematic model exhibits the dynamical formation, via topcolor, of the Higgs doublet as a composite field of the form:

$$\varphi = \begin{pmatrix} \overline{\chi_R} t_L \\ \overline{\chi_R} b_L \end{pmatrix}. \quad (2.1)$$

We proceed by introducing an embedding of QCD into the gauge groups $SU(3)_1 \times SU(3)_2$, with coupling constants h_1 and h_2 respectively. These symmetry groups are broken down to $SU(3)_{QCD}$ at a high mass scale \mathcal{V} . The assignment of the elementary fermions to representations under the full set of gauge groups $SU(3)_1 \times SU(3)_2 \times SU(2)_W \times U(1)_Y$ is as follows:

$$\psi_L : (\mathbf{3}, \mathbf{1}, \mathbf{2}, +1/3) \quad , \quad \chi_R : (\mathbf{3}, \mathbf{1}, \mathbf{1}, +4/3) \quad , \quad t_R, \chi_L : (\mathbf{1}, \mathbf{3}, \mathbf{1}, +4/3). \quad (2.2)$$

This set of fermions is incomplete: the representation specified has $[SU(3)_1]^3$, $[SU(3)_2]^3$, and $U(1)_Y[SU(3)_{1,2}]^2$ gauge anomalies. These anomalies will be canceled by fermions associated with either the dynamical breaking of $SU(3)_1 \times SU(3)_2$, or with producing the b -quark mass (a specific example of the latter case is given at the end of this section). The dynamics of EWSB and top-quark mass generation will not depend on the details of these additional fermions.

We further introduce a scalar field, Φ , transforming as $(\overline{\mathbf{3}}, \mathbf{3}, \mathbf{1}, 0)$, with negative M_Φ^2 and an associated quartic potential such that Φ develops a diagonal VEV,

$$\langle \Phi_j^i \rangle = \mathcal{V} \delta_j^i, \quad (2.3)$$

and topcolor is broken to QCD:

$$SU(3)_1 \times SU(3)_2 \longrightarrow SU(3)_{QCD} , \quad (2.4)$$

yielding massless gluons and an octet of degenerate colorons with mass M given by:

$$M^2 = (h_1^2 + h_2^2) \mathcal{V}^2 . \quad (2.5)$$

In more complete models this symmetry breaking may arise dynamically, but we describe it in terms of a VEV of a fundamental scalar field in the present model for the sake of simplicity.

We now introduce a Yukawa coupling of the fermions $\chi_{L,R}$ to Φ of the form:

$$- \xi \overline{\chi}_R \Phi \chi_L + \text{h.c.} \longrightarrow -\mu_{\chi\chi} \overline{\chi}\chi \quad (2.6)$$

We emphasize that this is an electroweak singlet mass term. In this scheme ξ is a perturbative coupling constant so $\mathcal{V} \gg \mu_{\chi\chi}$. Finally, since both t_R and χ_L carry identical topcolor and $U(1)_Y$ quantum numbers we are free to include an explicit mass term, also an electroweak singlet, of the form:

$$- \mu_{\chi t} \overline{\chi}_L t_R + \text{h.c.} \quad (2.7)$$

The mass terms of $\overline{\chi}_L \chi_R$ and $\overline{\chi}_L t_R$ may arise dynamically in subsequent schemes, and are introduced by hand into the schematic model for purposes of illustration. With these terms, the Lagrangian of the model at scales below the coloron mass is $SU(3)_C \times SU(2)_W \times U(1)$ invariant and becomes:

$$\mathcal{L}_0 = \mathcal{L}_{\text{kinetic}} - (\mu_{\chi\chi} \overline{\chi}_L \chi_R + \mu_{\chi t} \overline{\chi}_L t_R + \text{h.c.}) + \mathcal{L}_{\text{int}} \quad (2.8)$$

\mathcal{L}_{int} contains the residual topcolor interactions from the exchange of the massive colorons:

$$\mathcal{L}_{\text{int}} = -\frac{g_{tc}^2}{M^2} \left(\overline{\psi}_L \gamma^\mu \frac{\lambda^A}{2} \psi_L \right) \left(\overline{\chi}_R \gamma_\mu \frac{\lambda^A}{2} \chi_R \right) + LL + RR , \quad (2.9)$$

where LL (RR) refers to left-handed (right-handed) current-current interactions, and g_{tc} is the topcolor gauge coupling. Since the topcolor interactions are strongly coupled, forming boundstates, higher dimensional operators might have a significant effect on the low energy theory. However, if the full topcolor dynamics induces chiral symmetry breaking through a second order (or weakly first order) phase transition, then one can analyze the theory using the fundamental degrees of freedom, namely the quarks, at scales significantly lower

than the topcolor scale. We will assume that this is the case, which implies that the effects of the higher dimensional operators are suppressed by powers of the topcolor scale, and it is sufficient to keep in the low energy theory only the effects of the operators shown in eq. (2.9). Furthermore, the LL and RR interactions do not affect the low-energy effective potential in the large N_c limit [8], so we will ignore them (one should keep in mind that these interactions may have other effects, such as contributions to the custodial symmetry violation parameter T [9, 8], but these effects are negligible if the topcolor scale is in the multi-TeV range).

To leading order in $1/N_c$, the LR interaction in (2.9) can be rearranged into the following form:

$$\mathcal{L}_{\text{int}} = \frac{g_{\text{tc}}^2}{M^2} (\overline{\psi}_L \chi_R) (\overline{\chi}_R \psi_L) . \quad (2.10)$$

This is the Nambu-Jona-Lasinio (NJL) interaction [10], which provides the binding of the composite Higgs multiplet. We will analyze the physics of (2.8) by using the coloron mass M as a momentum space cut-off on the loop integrals of the theory.

It is convenient to pass to a mass eigenbasis with the following redefinitions:

$$\begin{aligned} \chi'_R &= \cos \theta \chi_R + \sin \theta t_R , \\ t'_R &= \cos \theta t_R - \sin \theta \chi_R , \end{aligned} \quad (2.11)$$

where:

$$\tan \theta = \frac{\mu_{\chi t}}{\mu_{\chi\chi}} \quad (2.12)$$

In this basis, the NJL Lagrangian takes the form:

$$\begin{aligned} \mathcal{L}_0 &= \mathcal{L}_{\text{kinetic}} - \overline{M} \overline{\chi}'_R \chi_L + \text{h.c.} \\ &+ \frac{g_{\text{tc}}^2}{M^2} \left[\overline{\psi}_L (\cos \theta \chi'_R - \sin \theta t'_R) \right] \left[(\cos \theta \overline{\chi}'_R - \sin \theta \overline{t}'_R) \psi_L \right] \end{aligned} \quad (2.13)$$

where

$$\overline{M} = \sqrt{\mu_{\chi\chi}^2 + \mu_{\chi t}^2} . \quad (2.14)$$

We now proceed with the analysis by factoring the interaction term in (2.13) by introducing a static auxiliary color-singlet field, φ_0 (which will become the *unrenormalized* composite Higgs doublet), to obtain:

$$\mathcal{L}_0 = \mathcal{L}_{\text{kinetic}} - \left[\overline{M} \overline{\chi}'_R \chi_L + g_{\text{tc}} \overline{\psi}_L (\cos \theta \chi'_R - \sin \theta t'_R) \varphi_0 + \text{h.c.} \right] - M^2 \varphi_0^\dagger \varphi_0 . \quad (2.15)$$

We now derive the low energy effective Lagrangian by means of the block-spin renormalization group. We view eq. (2.15) as the effective Lagrangian of the theory at a distance scale $\sim 1/M$. To derive the effective Lagrangian at a larger distance scale, $\sim 1/\mu$, where $M > \mu$, we integrate out the modes of momenta $M \geq |k| \geq \mu$. For $M > \bar{M} > \mu$ the field χ decouples, and we obtain:

$$\mathcal{L}_{\bar{M} > \mu} = \mathcal{L}_{\text{kinetic}} - g_{tc} \sin \theta \left(\overline{\psi}_L t'_R \varphi_0 + \text{h.c.} \right) + Z_\varphi |D\varphi_0|^2 - \widetilde{M}_\varphi^2(\mu) \varphi_0^\dagger \varphi_0 - \widetilde{\lambda} \left(\varphi_0^\dagger \varphi_0 \right)^2 \quad (2.16)$$

In the limit $M > \bar{M} > \mu$, we obtain by integrating the fermion loops:

$$\begin{aligned} \widetilde{M}_\varphi^2(\mu) &= M^2 - \frac{g_{tc}^2 N_c}{8\pi^2} \left[M^2 - \cos^2 \theta \bar{M}^2 \ln \left(\frac{M^2}{\bar{M}^2} \right) \right] + \mathcal{O}(\bar{M}^2, \mu^2) , \\ Z_\varphi &= \frac{g_{tc}^2 N_c}{16\pi^2} \left[\ln \left(\frac{M^2}{\bar{M}^2} \right) + \ln \left(\frac{\bar{M}^2}{\mu^2} \right) \sin^2 \theta + \mathcal{O}(1) \right] , \\ \widetilde{\lambda} &= \frac{g_{tc}^4 N_c}{8\pi^2} \left[\ln \left(\frac{M^2}{\bar{M}^2} \right) + \ln \left(\frac{\bar{M}^2}{\mu^2} \right) \sin^4 \theta + \mathcal{O}(1) \right] . \end{aligned} \quad (2.17)$$

These relationships are true for $\bar{M} > \mu$ in the large N_c approximation, and illustrate the decoupling of the χ field at the scale \bar{M} . In the limit $\sin \theta \ll 1$ we see that the induced couplings are those of the usual NJL model. However, in this limit the Higgs doublet is predominantly a boundstate of $\overline{\chi}_R \psi_L$, and the corresponding loop, with loop-momentum ranging over $M > |k| > \bar{M}$, controls most of the renormalization group evolution of the effective Lagrangian.

Consider, therefore, the limit $\sin^2 \theta \ll 1$, hence $\cos^2 \theta \approx 1$. In order for the composite Higgs doublet to develop a VEV, the $SU(3)_1$ interaction must be supercritical. The criticality condition corresponds to demanding a negative $\widetilde{M}_\varphi^2(\mu)$ as $\mu \rightarrow 0$:

$$\frac{g_{tc}^2 N_c}{8\pi^2} \geq \left[1 - \frac{\mu_{\chi\chi}^2}{M^2} \ln \left(\frac{M^2}{\mu_{\chi\chi}^2} \right) \right]^{-1} \quad (2.18)$$

This condition is equivalent to the NJL criticality condition for $\mu_{\chi\chi}^2/M^2 \ll 1$. Once we take g to be supercritical, we are free to tune the renormalized Higgs boson mass, $M_\varphi^2(\mu) = \widetilde{M}_\varphi^2(\mu)/Z_\varphi$, to any desired value. This implies that we are free to adjust the renormalized VEV of the Higgs doublet to the electroweak value, $\langle \varphi^0 \rangle = v/\sqrt{2} \approx 175$ GeV. The effective Lagrangian at low energies, written in terms of the renormalized field φ , takes the form:

$$\mathcal{L}_{\bar{M} > \mu} = \mathcal{L}_{\text{kinetic}} - g_t \sin \theta \left(\overline{\psi}_L t'_R \varphi + \text{h.c.} \right) + |D\varphi|^2 - M_\varphi^2(\mu) \varphi^\dagger \varphi - \lambda (\varphi^\dagger \varphi)^2 \quad (2.19)$$

where:

$$\varphi = \varphi_0 \sqrt{Z_\varphi}; \quad g_t = \frac{g_{tc}}{\sqrt{Z_\varphi}}; \quad M_\varphi^2(\mu) = \frac{\widetilde{M}_\varphi^2(\mu)}{Z_\varphi}; \quad \lambda = \frac{\widetilde{\lambda}}{Z_\varphi^2}. \quad (2.20)$$

The resulting top quark mass can be read off from the renormalized Lagrangian:

$$m_t = g_t \sin \theta \frac{v}{\sqrt{2}}, \quad (2.21)$$

which corresponds to a Pagels-Stokar formula of the form:

$$v^2 = \frac{N_c}{8\pi^2} \frac{m_t^2}{\sin^2 \theta} \ln \left(\frac{M^2}{M^2} \right) + \mathcal{O}(\sin^2 \theta). \quad (2.22)$$

The Pagels-Stokar formula differs from that obtained (in large N_c approximation) for top quark condensation models by the large enhancement factor $1/\sin^2 \theta$. This is a direct consequence of the seesaw mechanism.

We note that, in principle, using the freedom to adjust $\sin \theta$ we could accommodate any fermion mass lighter than 600 GeV. This freedom may be useful in constructing more complete models involving all three generations. The top quark is unique, however, in that it is very difficult to accommodate such a heavy quark in any other way. We therefore believe it is generic, in any model of this kind, that the top quark receives the bulk of its mass through this seesaw mechanism.

To better understand the connection to the seesaw mechanism we can view the dynamics of the top quark mass from the mixing with the χ field. The mass matrix for the heavy charge 2/3 quarks takes the form:

$$\begin{pmatrix} \overline{t}_L & \overline{\chi}_L \end{pmatrix} \begin{pmatrix} 0 & m_{t\chi} \\ \mu_{\chi t} & \mu_{\chi\chi} \end{pmatrix} \begin{pmatrix} t_R \\ \chi_R \end{pmatrix}. \quad (2.23)$$

where $m_{t\chi}$ is dynamically generated by the VEV of the composite Higgs, φ , thus satisfying the Pagels-Stokar relationship:

$$v^2 = \frac{N_c}{8\pi^2} m_{t\chi}^2 \ln \left(\frac{M^2}{\mu_{\chi\chi}^2} \right). \quad (2.24)$$

If the logarithm is not very large, then we obtain the advertised value $m_{t\chi} \sim 600$ GeV. Diagonalizing the fermionic mass matrix of (2.23) for $\mu_{\chi\chi} \gg m_{t\chi}$ leads to the physical top mass:

$$m_t \approx \frac{m_{t\chi} \mu_{\chi t}}{\mu_{\chi\chi}} = m_{t\chi} \tan \theta, \quad (2.25)$$

and substitution of (2.25) into (2.24) reproduces (2.22) for small $\tan \theta \approx \sin \theta$.

The minimization of the Higgs potential gives the usual NJL result, that the Higgs boson has a mass twice as large as the dynamically generated fermion mass, which is $m_{t\chi}$ in the present case. Thus, the schematic model includes only one composite Higgs boson, which is heavy, of order 1 TeV. In Section 3.4 we will show that in a more general theory that includes the seesaw mechanism there are more composite scalars, and one of the neutral Higgs bosons may be as light as $\mathcal{O}(100 \text{ GeV})$.

We note that the inclusion of the b -quark is straightforward, and the schematic model affords a simple way to suppress the formation of a b -quark mass comparable to the top quark mass. We include additional fermionic fields of the form ω_L , ω_R , and b_R with the assignments:

$$b_R, \omega_L : (\mathbf{1}, \mathbf{3}, \mathbf{1}, -2/3) \quad , \quad \omega_R : (\mathbf{3}, \mathbf{1}, \mathbf{1}, -2/3) \quad . \quad (2.26)$$

These fermion gauge assignments cancel the anomalies noted above. We further allow $\overline{\omega}_L \omega_R$ and $\overline{\omega}_L b_R$ mass terms, in direct analogy to the χ and t mass terms:

$$\mathcal{L}_0 \supset -(\mu_{\omega\omega} \overline{\omega}_L \omega_R + \mu_{\omega b} \overline{\omega}_L b_R + \text{h.c.}) \quad (2.27)$$

We can suppress the formation of the $\overline{\omega}_L b_R$ condensate altogether by choosing $\overline{M}_\omega = \sqrt{\mu_{\omega\omega}^2 + \mu_{\omega b}^2} \sim M$. In this limit we do not produce a b -quark mass. However, by allowing $\mu_{\omega\omega} \leq M$ and $\mu_{\omega b}/\mu_{\omega\omega} \ll 1$ we can form an acceptable b -quark mass in the presence of a small $\overline{\omega}_L b_R$ condensate. Yet another possibility arises within this model, though it will not be a general feature of these schemes, i.e., to exploit instantons [5]. If we suppress the formation of the $\overline{\omega}_L b_R$ condensate by choosing $\overline{M}_\omega \sim M$, there will be a $\overline{\omega}_L b_R$ condensate induced via the 't Hooft determinant when the t and χ are integrated out. We then estimate the scale of the induced $\overline{\omega}_L b_R$ mass term to be about $\sim 20 \text{ GeV}$, and the b -quark mass then emerges as $\sim 20\mu_{\omega b}/\mu_{\omega\omega} \text{ GeV}$. We will not further elaborate the b -quark mass in the present discussion, since its precise origin depends critically upon the structure of the complete theory including all light quarks and leptons.

3 The Effective Potential Formalism

3.1 More General Interactions

Presently we extend the schematic model to include various additional interactions, beyond the topcolor interaction of eq. (2.9). While we would ultimately like to replace the $\mu_{\chi\chi}$ and $\mu_{\chi t}$ explicit mass terms exclusively with additional strong dynamics, we find

presently that is not possible without the inclusion of additional fields and additional dynamics. The seesaw mechanism, at least in the large- N_c fermion loop approximations seems to require these terms, and they also lift unwanted massless Nambu-Goldstone bosons. In Section 4 we will sketch out a more general high energy theory in which these masses may arise dynamically, in analogy to extended technicolor. However, in the present case, these mass terms will be viewed as “small,” in contrast to the schematic model in which they were large.

The NJL approximation illustrated in Section 2 is probably a reasonable guide to the physics of topcolor. One can frame the discussion in terms of “gap equations” and their solutions, as in [3], but it is useful and convenient to have a more general and detailed description. In particular, the vacuum structure of the topcolor theory is crucial to the success of the enterprise, and it is important to study it with all the tools at our disposal. One of the most useful tools is the effective potential [11]. This has been used in [1] to analyze simple topcolor models, and it was employed in Section 2 in eqs. (2.16) and (2.17) in lieu of the exclusive use of gap equations as in [3]. In this Section we extend its use in the present seesaw scheme involving additional strong interactions .

We thus consider a low energy effective theory, valid up to a scale $M > O(10 \text{ TeV})$, consisting of the standard model gauge group and fermions, and a new vectorlike quark, χ , which transforms under the $SU(3)_C \times SU(2)_W \times U(1)_Y$ gauge group exactly as the right-handed top, t_R .

We assume that at the common scale M the following four-fermion, NJL-like interactions, involving the top, bottom and vectorlike quarks, occur:

$$\mathcal{L}_{\text{int}} = \frac{8\pi^2}{N_c M^2} \sum_{A,B=b,t,\chi} z_{AB} (\bar{A}_L B_R) (\bar{B}_R A_L) , \quad (3.1)$$

where $N_c = 3$ is the numbers of colors. The z_{AB} ($A, B = b, t, \chi$) are dynamical coefficients determined by the couplings of the high energy theory. At the scale M the electroweak symmetry is unbroken, implying $z_{bA} = z_{tA}$. Hence there are six independent z_{AB} coefficients. Our normalization is chosen so that the interaction strength will be approximately critical (subcritical) in the AB channel when $z_{AB} > 1$ ($z_{AB} < 1$). The interactions of eq. (3.1) should be viewed as Fierz-rearranged versions of single massive gauge boson exchange interactions arising in a more general high energy theory. For example, we imagine that the four-fermion operators (3.1) arise from topcolor-like [4] interactions, and therefore z_{AB} are functions of gauge couplings and charges. In the special case of the schematic model of Section 2, $z_{t\chi} = N_c g_{tc}^2 / (8\pi^2)$ and all other z_{AB} coefficients

are zero. In the model introduced in ref. [3] all $z_{AB} \sim 1$, and their dependence upon the charges is given in the present paper in Appendix A [see eq. (A.1)].

In addition to the four-fermion operators (3.1), small, explicit, electroweak preserving mass terms are allowed in the Lagrangian:

$$\mathcal{L}_{\text{mass}} = -\mu_{\chi\chi}\bar{\chi}_L\chi_R - \mu_{\chi t}\bar{\chi}_L t_R + \text{h.c.} \quad (3.2)$$

The model presented in Section 4 is an example of high energy physics that generates dynamically these four-fermion operators and masses.

3.2 The Effective Potential

The four-fermion interactions can be factorized, at the scale M , by introducing static auxiliary fields $\phi_{0AB} \equiv \bar{B}_R A_L$ ($A, B = b, t, \chi$), which are described by the following effective Lagrangian:

$$\begin{aligned} \mathcal{L}_{\text{eff}} = & \sum_{A,B=b,t,\chi} \left[\left(\bar{A}_L B_R \phi_{0AB} + \text{h.c.} \right) + \frac{N_c M^2}{8\pi^2 z_{AB}} \phi_{0AB}^\dagger \phi_{0AB} \right] \\ & - (\mu_{\chi\chi}\bar{\chi}_L\chi_R + \mu_{\chi t}\bar{\chi}_L t_R + \text{h.c.}) . \end{aligned} \quad (3.3)$$

At the scale M , the ϕ_{0AB} have vanishing kinetic terms. At scales below M the ϕ_{0AB} will acquire kinetic terms through the effects of fermion loops and become propagating composite scalar fields. The loops also generally induce running mass terms and running quartic and Yukawa interactions. The fields are renormalized $\phi_{0AB} \rightarrow \phi_{AB}$, to give conventional kinetic term normalizations, and we thus find at a scale $\mu < M$, using, e.g., block spin renormalization group in the large N_c approximation, the effective Lagrangian:

$$\mathcal{L}_{\text{eff}}^\mu = g_t \sum_{A,B=b,t,\chi} \left(\bar{A}_L B_R \phi_{AB} + \text{h.c.} \right) + \left(D_\nu \phi_{AB}^\dagger \right) \left(D^\nu \phi_{AB} \right) - V(\phi) . \quad (3.4)$$

Here we redefined the renormalized scalar fields by including a shift to absorb the explicit mass fermionic terms:

$$\phi_{AB} \equiv \phi_{0AB} \sqrt{Z_\phi} - \frac{\mu_{AB}}{g_t} , \quad (3.5)$$

where Z_ϕ is the wave function renormalization, and $\mu_{AB} = 0$, except for $\mu_{\chi\chi}$ and $\mu_{\chi t}$. In the large N_c limit, the one-loop effective potential is given by:

$$V(\phi) = \frac{\lambda}{2} \text{Tr} \left[\left(\phi^\dagger \phi \right)^2 \right] + \sum_{A,B=b,t,\chi} \left[M_{AB}^2 \phi_{AB}^\dagger \phi_{AB} + C_{AB} \left(\phi_{AB} + \phi_{AB}^\dagger \right) \right] . \quad (3.6)$$

Note that the trace is just the sum over repeated indices of $\phi_{AB}^\dagger \phi_{BC} \phi_{CD}^\dagger \phi_{DA}$. The renormalized quartic and Yukawa coupling constants depend logarithmically on the physical cut-off,

$$g_t = \sqrt{\frac{\lambda}{2}} = \frac{4\pi}{\sqrt{N_c \ln(M^2/\mu^2)}} , \quad (3.7)$$

while the scalar squared-masses and tadpole coefficients depend quadratically on M :

$$\begin{aligned} M_{AB}^2 &= \frac{2M^2}{\ln(M^2/\mu^2)} \left(\frac{1}{z_{AB}} - 1 \right) , \\ C_{AB} &= \frac{\mu_{AB} M^2}{2\pi z_{AB}} \sqrt{\frac{N_c}{\ln(M^2/\mu^2)}} > 0 . \end{aligned} \quad (3.8)$$

Note that with our conventions the C_{AB} are positive and electroweak symmetry imposes $C_{Ab} = C_{tt} = C_{t\chi} = 0$. This is just the usual effective potential derivation as in [1] applied to the present more general interaction.

In order to determine the vacuum properties of the theory we minimize the effective potential. Note that a global $U(1)_{b_R}$ symmetry forbids tadpole terms for the ϕ_{Ab} scalars, independent of the VEVs of the other scalars. We further assume that the Ab channels are subcritical, thus:

$$z_{Ab} < 1 , \quad A = b, t, \chi , \quad (3.9)$$

so that $M_{Ab}^2 > 0$. As a result, the composite scalars having b_R as constituents do not acquire VEVs: $\langle \phi_{Ab} \rangle = 0$. An $SU(2)_W$ transformation allows us to set $\langle \phi_{b\chi} \rangle = 0$. We also take $z_{tt} < 1$, such that $M_{tt}^2 > 0$, which implies that ϕ_{bt} and ϕ_{tt} may acquire VEVs only if they have tadpole terms induced by the VEVs of the other scalars. This implies that the VEVs of the $SU(2)_W$ doublet scalars, $\bar{t}_R \psi_L$ and $\bar{\chi}_R \psi_L$, are aligned, so that $\langle \phi_{bt} \rangle = 0$. Finally, it is obvious that a nonzero VEV for $\phi_{t\chi}$ requires $M_{t\chi}^2 < 0$, while the signs and sizes of $M_{\chi t}^2$ and $M_{\chi\chi}^2$ are not constrained so far.

Altogether only four out of the nine composite fields may have nonzero VEVs: $\langle \phi_{AB} \rangle$ with $A, B = \chi, t$. At the minimum of the effective potential (3.6), the phases of the $\phi_{\chi\chi}$ and $\phi_{\chi t}$ are forced to be -1 by the tadpole terms (recall that the electroweak symmetry imposes $C_{tt} = C_{t\chi} = 0$). In addition, the relative phase between $\langle \phi_{t\chi} \rangle$ and $\langle \phi_{tt} \rangle$ has to be negative in order to minimize the quartic terms in the effective potential. Thus, there is only one arbitrary phase left, which can be fixed by choosing $\langle \phi_{tt} \rangle > 0$. Let us denote the absolute values of the VEVs by v_{AB} , so that:

$$v_{tt} = \langle \phi_{tt} \rangle , \quad v_{\chi\chi} = -\langle \phi_{\chi\chi} \rangle , \quad v_{t\chi} = -\langle \phi_{t\chi} \rangle , \quad v_{\chi t} = -\langle \phi_{\chi t} \rangle . \quad (3.10)$$

The values of v_{AB} can be determined by minimizing the following function:

$$\begin{aligned}
V(v_{AB}) &= \frac{\lambda}{2} \left[(v_{tt}^2 + v_{t\chi}^2)^2 + (v_{\chi\chi}^2 + v_{\chi t}^2)^2 + 2(v_{tt}v_{\chi t} - v_{\chi\chi}v_{t\chi})^2 \right] \\
&+ \sum_{A,B=t,\chi} M_{AB}^2 v_{AB}^2 - 2C_{\chi\chi}v_{\chi\chi} - 2C_{\chi t}v_{\chi t} .
\end{aligned} \tag{3.11}$$

We would like to find a vacuum that satisfies a general seesaw condition. It is convenient to parametrize the VEVs as follows (up to phases and an overall factor of g_t , this is just the fermionic mass matrix):

$$\begin{pmatrix} v_{tt} & v_{t\chi} \\ v_{\chi t} & v_{\chi\chi} \end{pmatrix} = v_{\chi\chi} \begin{pmatrix} ab\epsilon & \epsilon \\ b & 1 \end{pmatrix} . \tag{3.12}$$

In terms of the dimensionless parameters a , b and ϵ introduced here, the general seesaw condition reads:

$$0 < \epsilon < b < 1 , \quad 0 < a \ll \frac{1}{\epsilon} , \quad \epsilon \ll 1 . \tag{3.13}$$

The limit $a, b \ll 1$ corresponds to the seesaw condition used in ref. [3]. One can easily check that the stationarity conditions,

$$\frac{\partial V}{\partial v_{AB}} = 0 , \quad A, B = t, \chi , \tag{3.14}$$

have indeed a solution satisfying eqs. (3.13). This solution is a stable minimum of the effective potential if and only if all four eigenvalues of the second derivative of V are positive at the stationary point. Before computing the eigenvalues, we note that the equations $\partial V/\partial v_{\chi\chi} = 0$ and $\partial V/\partial v_{\chi t} = 0$ give ϵ and b in terms of $C_{\chi\chi}$, $C_{\chi t}$ and M_{AB}^2 . As a consequence, the conditions $C_{\chi\chi}, C_{\chi t} > 0$, used in fixing the phases of the VEVs, impose the following restrictions:

$$M_{\chi t}^2, M_{\chi\chi}^2 > M_{t\chi}^2 \frac{1+b^2}{1-\rho b^2} \left[1 + \mathcal{O}(\epsilon^2) \right] , \tag{3.15}$$

where we defined:

$$\rho \equiv \frac{-M_{t\chi}^2}{M_{tt}^2} > 0 . \tag{3.16}$$

The other two stationarity conditions, $\partial V/\partial v_{tt} = 0$ and $\partial V/\partial v_{t\chi} = 0$, yield:

$$\begin{aligned}
a &= \rho \left[1 + \mathcal{O}(\epsilon^2) \right] , \\
v_{\chi\chi}^2 &= \frac{-M_{t\chi}^2}{\lambda(1-\rho b^2)} \left[1 - \epsilon^2(1+\rho^2 b^2) \frac{1-\rho(1-2\rho)b^2}{(1-\rho b^2)^2} + \mathcal{O}(\epsilon^4) \right] .
\end{aligned} \tag{3.17}$$

These expressions allow us to write the second derivative of $V(v_{AB})$ as the following 4×4 matrix:

$$\partial^2 V(v_{AB}) = 2\lambda v_{\chi\chi}^2 \begin{pmatrix} \mathcal{A}_1 + \epsilon^2 \mathcal{B}_1 + \mathcal{O}(\epsilon^4) & \epsilon \mathcal{B}_3 + \mathcal{O}(\epsilon^3) \\ \epsilon \mathcal{B}_3^\top + \mathcal{O}(\epsilon^3) & \mathcal{A}_2 + \epsilon^2 \mathcal{B}_2 + \mathcal{O}(\epsilon^4) \end{pmatrix}, \quad (3.18)$$

where $\mathcal{A}_{1,2}$ and $\mathcal{B}_{1,2,3}$ are 2×2 real matrices that depend only on b and $M_{tt,tx,xt,xx}^2$. Note that the rows and columns of $\partial^2 V(v_{AB})$ are arranged in eq. (3.18) in the following order: $v_{tt}, v_{t\chi}, v_{\chi t}, v_{\chi\chi}$. Using the explicit form of $\mathcal{A}_{1,2}$,

$$\begin{aligned} \mathcal{A}_1 &= \begin{pmatrix} 1/\rho & -b \\ -b & \rho b^2 \end{pmatrix}, \\ \mathcal{A}_2 &= \left(\frac{1 - \rho b^2}{-M_{t\chi}^2} \right) \text{diag} \left(M_{\chi\chi}^2, M_{\chi t}^2 \right) + \begin{pmatrix} 3 + b^2 & 2b \\ 2b & 1 + 3b^2 \end{pmatrix}, \end{aligned} \quad (3.19)$$

it is easy to compute to first order in ϵ^2 the eigenvalues of $\partial^2 V(v_{AB})$. Three of these are positive [eq. (3.15) is important here], while the fourth eigenvalue cancels to leading order in ϵ^2 . To ensure vacuum stability, the corrections of order ϵ^2 to $\partial^2 V$ must give a positive contribution to this eigenvalue. We check this condition in Section 3.4, where we also show that this eigenvalue corresponds to the mass of a light Higgs boson.

3.3 Parameter Space

The effective potential depends on six squared-masses $M_{tA}^2, M_{\chi A}^2$ ($A = b, t, \chi$), two tadpole coefficients $C_{\chi\chi}, C_{\chi t}$, and on $\ln(M/\mu)$. We will choose the renormalization point μ to be the mass of the χ fermion. In doing so, we will neglect the running of the coefficients in the effective potential between the scale m_χ and the scale m_t . In practice, this approximation is justified only if $M/m_\chi > m_\chi/m_t \sim 1/\epsilon$. We emphasize that this condition is not needed in a more developed computation of the renormalization group evolution.

We will proceed with deriving the constraints imposed on the parameters of the effective potential by the measured values of the W , Z and t masses. The elements of the fermion mass matrix are proportional to the VEVs:

$$m_{AB} = -g_t \langle \phi_{AB} \rangle. \quad (3.20)$$

It is straightforward to compute the top and χ quark masses [see eq. (B.2)]:

$$m_t = m_{t\chi} \frac{b(1+\rho)}{\sqrt{1+b^2}} \left[1 + \mathcal{O}(\epsilon^2) \right],$$

$$m_\chi = \frac{m_{t\chi}}{\epsilon} \sqrt{1+b^2} \left[1 + \frac{\epsilon^2}{2} \left(\frac{1-\rho b^2}{1+b^2} \right)^2 + \mathcal{O}(\epsilon^4) \right]. \quad (3.21)$$

The electroweak symmetry is broken only by the VEVs of $\phi_{\psi\chi}$ and $\phi_{\psi t}$,

$$\frac{v^2}{2} = v_{t\chi}^2 + v_{tt}^2, \quad (3.22)$$

which implies:

$$\begin{aligned} m_{t\chi} &= \frac{g_t v}{\sqrt{2(1+\rho^2 b^2)}} \left[1 + \mathcal{O}(\epsilon^2) \right] \\ &\approx 890 \text{ GeV} \left[(1+\rho^2 b^2) \ln \left(\frac{M}{m_\chi} \right) \right]^{-1/2}. \end{aligned} \quad (3.23)$$

Using the expression for the top quark mass in eq. (3.21), we find a constraint on b and ρ ,

$$\frac{b^2(1+\rho)^2}{(1+b^2)(1+\rho^2 b^2)} \approx 4 \times 10^{-2} \ln \left(\frac{M}{m_\chi} \right), \quad (3.24)$$

which shows that $b^2 \lesssim \mathcal{O}(0.1)$ (M is not larger by many orders of magnitude than m_χ unless the coefficients of the four-fermion operators are excessively fine-tuned to be close to the critical value).

The χ'_L mass eigenstate couples to W and Z so that there is a potentially large custodial symmetry violation. However, in the decoupling limit ($\epsilon/b \rightarrow 0$) this effect vanishes. To show this we consider the one-loop contribution of χ to the T parameter:

$$T = \frac{3}{16\pi^2 \alpha v^2} \left[s_L^4 m_\chi^2 + 2s_L^2(1-s_L^2) \frac{m_\chi^2 m_t^2}{m_\chi^2 - m_t^2} \ln \left(\frac{m_\chi^2}{m_t^2} \right) - s_L^2(2-s_L^2) m_t^2 \right], \quad (3.25)$$

where s_L is the sine of the left-handed mixing angle, defined in eq. (B.4):

$$s_L = \epsilon \left[1 - b^2 \frac{(1+\rho)(3-\rho)}{2(1+b^2)} \right]^{1/2} + \mathcal{O}(\epsilon^3). \quad (3.26)$$

Because this mixing is small, the χ loop contribution to T is suppressed compared to the top loop contribution by a factor of ϵ^2/b^2 :

$$T = \frac{N_c m_t^2}{16\pi^2 \alpha (M_Z^2) v^2} \frac{\epsilon^2}{b^2} \left[1 - 4b^2 \ln(\epsilon b) \right] \left[1 + \mathcal{O}(b^2, \epsilon^2) \right]. \quad (3.27)$$

In practice, the current experimental constraints on T are satisfied if b is larger than ϵ by a factor of 2 or so [3]. Thus, the upper bound on ϵ is about 0.1, confirming that the expansion in ϵ^2 is a good approximation.

To summarize, for $M/m_\chi \sim 10$ the elements of the fermion mass matrix eq. (3.12) have sizes:

$$\begin{pmatrix} m_{tt} \lesssim \mathcal{O}(100 \text{ GeV}) & m_{t\chi} \sim \mathcal{O}(600 \text{ GeV}) \\ m_{\chi t} \gtrsim \mathcal{O}(1 \text{ TeV}) & m_{\chi\chi} \gtrsim \mathcal{O}(5 \text{ TeV}) \end{pmatrix}. \quad (3.28)$$

The effective potential analysis given is valid only for $M \gg m_{\chi\chi}$. Smaller values of M (with less fine-tuning) may be allowed, though we cannot demonstrate that fact. The relations between ϵ, b and $C_{\chi\chi}, C_{\chi t}$ allow us to estimate the $\mu_{\chi\chi}$ and $\mu_{\chi t}$ mass coefficients from the Lagrangian:

$$\mu_{\chi A} = m_{\chi A} \frac{M_{\chi A}^2 - M_{t\chi}^2}{2z_{\chi A} M^2} \ln \left(\frac{M}{m_\chi} \right) \left[1 + \mathcal{O}(b^2, \epsilon^2) \right]. \quad (3.29)$$

Generically we expect $|M_{AB}| \sim \mathcal{O}(m_\chi) < \epsilon M$, so that $\mu_{\chi A}/m_{\chi A} < \mathcal{O}(\epsilon^2)$. By contrast, in Section 2 the schematic model does not lead to a $\phi_{\chi t}$ or $\phi_{\chi\chi}$ bound state, and eq. (3.29) is replaced by $\mu_{\chi A} = m_{\chi A}$.

3.4 The Composite Scalar Spectrum

Next we compute the composite scalar spectrum. The 3×3 matrix ϕ contains a total of 18 real scalar degrees of freedom, corresponding potentially to a Higgs sector which includes three weak-doublets, $\phi_{\psi A} \equiv \bar{A}_R \psi_L$ with $A = b, t, \chi$ and $\psi_L = (t, b)_L$, and three weak-singlets, $\phi_{\chi A} \equiv \bar{A}_R \chi_L$.

An unbroken global $U(1)_{b_R}$ symmetry ensures that the $\phi_{\psi b}$ and $\phi_{\chi b}$ scalars do not mix with ϕ_{At} or $\phi_{A\chi}$. Therefore, the neutral complex scalar ϕ_{bb} has a mass M_{tb} given by eq. (3.8), and the complex scalars ϕ_{tb} and $\phi_{\chi b}$ with electric charge +1 have a mass matrix:

$$\text{diag} \left(M_{tb}^2, M_{\chi b}^2 \right) + \lambda v_{\chi\chi}^2 \begin{pmatrix} \epsilon^2(1 + a^2 b^2) & \epsilon(1 - ab^2) \\ \epsilon(1 - ab^2) & 1 + b^2 \end{pmatrix}. \quad (3.30)$$

In Section 3.2 we imposed $M_{tb}^2, M_{\chi b}^2 > 0$, which implies that the mixing between ϕ_{tb} and $\phi_{\chi b}$ is suppressed by ϵ . We will denote the mass eigenstates by H_{tb}^\pm and $H_{\chi b}^\pm$. The magnitudes of the masses that appear in the effective potential, $|M_{AB}|$, are expected to be roughly of the same order in the absence of fine-tuning. Using the relation:

$$\lambda v_{\chi\chi}^2 = \frac{2}{\epsilon^2} m_{t\chi}^2 \quad (3.31)$$

we can estimate $|M_{t\chi}|$ from eq. (3.17):

$$-M_{t\chi}^2 = \frac{2}{\epsilon^2} m_{t\chi}^2 \left(1 - \rho b^2 \right) \left[1 + \mathcal{O}(\epsilon^2) \right] \quad (3.32)$$

Given that $\rho b^2 \lesssim \mathcal{O}(0.1)$, as can be seen from eq. (3.24), it follows that $|M_{t\chi}| \gtrsim \mathcal{O}(5 \text{ TeV})$. If M_{tb} is indeed of the same order as $|M_{t\chi}|$, then the two charged scalars have masses of a few TeV or larger. On the other hand, if z_{tb} and $z_{\chi b}$ are tuned sufficiently close to one so that $M_{tb}, M_{\chi b} \ll b|M_{t\chi}|$, then the mass eigenstate which is predominantly ϕ_{tb} has a mass-squared:

$$M_{H_{tb}^\pm}^2 \approx 2m_t^2 + M_{tb}^2 . \quad (3.33)$$

This sets a lower bound on the charged Higgs mass of about 250 GeV.

The other two complex scalars with electric charges $+1$, ϕ_{bt} and $\phi_{b\chi}$ have the following mass matrix:

$$\text{diag} \left(M_{tt}^2, M_{t\chi}^2 \right) + \lambda v_{\chi\chi}^2 \begin{pmatrix} b^2(1 + a^2\epsilon^2) & b(1 - a\epsilon^2) \\ b(1 - a\epsilon^2) & 1 + \epsilon^2 \end{pmatrix} . \quad (3.34)$$

One of the eigenvalues vanishes, corresponding to the charged Nambu-Goldstone bosons that become the longitudinal W . The other eigenvalue is the mass-squared of a charged Higgs boson, H^\pm , and can be computed without expanding in powers of ϵ by using the stationarity conditions:

$$M_{H^\pm}^2 = \frac{2m_{t\chi}^2}{a\epsilon^2} (1 + a^2b^2)(1 - a\epsilon^2) . \quad (3.35)$$

This mass is also large, most likely above a TeV.

There are four CP-even neutral scalars, $\text{Re } \phi_{tt}$, $\text{Re } \phi_{t\chi}$, $\text{Re } \phi_{\chi\chi}$ and $\text{Re } \phi_{\chi t}$. Their mass matrix is given by:

$$\frac{1}{2} \text{diag}(1, -1, -1, -1) \partial^2 V(v_{AB}) \text{diag}(1, -1, -1, -1) , \quad (3.36)$$

with $\partial^2 V$ indicated in eq. (3.18). It is possible to compute the eigenvalues of this mass matrix as an expansion in ϵ^2 . There are two mass eigenstates which, to leading order in ϵ , are linear combinations of only $\text{Re } \phi_{tt}$ and $\text{Re } \phi_{t\chi}$. Since the electroweak symmetry is broken only by the VEVs of ϕ_{tt} and $\phi_{t\chi}$, it is appropriate to label these mass eigenstates by h^0 and H^0 , as in a two Higgs doublet model:

$$\begin{aligned} h^0 &= \sqrt{2} (1 + \rho b^2)^{-1/2} (\text{Re } \phi_{t\chi} + b\sqrt{\rho} \text{Re } \phi_{tt}) + \mathcal{O}(\epsilon) \\ H^0 &= \sqrt{2} (1 + \rho b^2)^{-1/2} (-b\sqrt{\rho} \text{Re } \phi_{t\chi} + \text{Re } \phi_{tt}) + \mathcal{O}(\epsilon) . \end{aligned} \quad (3.37)$$

The electroweak symmetry is unbroken in the $\epsilon \rightarrow 0$ limit, so that the heavy neutral Higgs boson is degenerate with H^\pm :

$$M_{H^0}^2 = \frac{2m_{t\chi}^2}{\rho\epsilon^2} (1 + \rho^2 b^2) [1 + \mathcal{O}(\epsilon^2)] = M_{H^\pm}^2 [1 + \mathcal{O}(\epsilon^2)] . \quad (3.38)$$

It is easier to compute the mass of the lightest neutral Higgs boson, M_{h^0} , as a power series in b^2 , which is a reasonably small parameter due to the constraint (3.24). The result is:

$$M_{h^0}^2 = 4m_{t\chi}^2 \frac{M_{\chi\chi}^2 - M_{t\chi}^2}{M_{\chi\chi}^2 - 3M_{t\chi}^2} [1 + \mathcal{O}(b^2, \epsilon^2)] . \quad (3.39)$$

For $M_{\chi\chi}^2 \sim -M_{t\chi}^2$, the h^0 is heavy, with a mass of order $\sqrt{2}m_{t\chi} \sim 800$ GeV. In the schematic model presented in Section 2, the $\phi_{\chi\chi}$ boundstate does not form, so that $M_{\chi\chi}^2 \rightarrow \infty$ and we recover the NJL result $M_{h^0} = 2m_{t\chi}$. On the other hand, if $M_{\chi\chi}^2 < 0$, the h^0 can be significantly lighter. A composite neutral Higgs boson with mass of order 100 GeV would require a cancellation between $M_{\chi\chi}^2$ and $M_{t\chi}^2$ at the level of 15%. Such a cancellation does not necessarily require fine-tuning: for instance, if ψ_L and χ_L have the same charges under the broken gauge groups that induce the four-fermion operators, then $z_{\chi\chi} = z_{t\chi}$ implying $M_{\chi\chi} = M_{t\chi}$. This shows that the existence of a light composite neutral Higgs boson, with a mass of order 100 GeV is a possibility.

To leading order in ϵ , the other two CP-even neutral mass eigenstates are linear combinations of $\text{Re } \phi_{\chi\chi}$ and $\text{Re } \phi_{\chi t}$, with a mixing of order b . Their squared-masses are given by:

$$\begin{aligned} M_{H_{\chi t}^0}^2 &= \frac{2}{\epsilon^2} m_{t\chi}^2 \left(1 + \frac{M_{\chi t}^2}{-M_{t\chi}^2} \right) [1 + \mathcal{O}(b^2, \epsilon^2)] , \\ M_{H_{\chi\chi}^0}^2 &= \frac{2}{\epsilon^2} m_{t\chi}^2 \left(3 + \frac{M_{\chi\chi}^2}{-M_{t\chi}^2} \right) [1 + \mathcal{O}(b^2, \epsilon^2)] . \end{aligned} \quad (3.40)$$

The $H_{\chi\chi}^0$ is heavy, with a mass of at least $\mathcal{O}(5 \text{ TeV})$, while $H_{\chi t}^0$ can be light, with a mass of order $m_{t\chi}$ or lower, if $M_{\chi t}^2$ and $M_{\chi\chi}^2$ are close to their lower bound (3.15). It is clear now that for typical values of the parameters in the effective potential all four CP-even neutral mass eigenstates have positive squared-masses, which proves that the minimization of the effective potential performed in Section 3.2 is correct. On the other hand, if the restriction (3.15) on $M_{\chi t}^2$ and $M_{\chi\chi}^2$ is saturated at order ϵ^2 , then the masses of $H_{\chi t}^0$ or h^0 might vanish, signaling a second order phase transition to an unacceptable vacuum.

The remaining four states are the CP-odd neutral scalars: $\text{Im } \phi_{tt}$, $\text{Im } \phi_{t\chi}$, $\text{Im } \phi_{\chi\chi}$ and $\text{Im } \phi_{\chi t}$. In the $\epsilon \rightarrow 0$ limit the masses of the $\phi_{\psi t}$ and $\phi_{\psi\chi}$ doublets are $SU(2)_W$ invariant,

so that the linear combination of $\text{Im } \phi_{tt}$ and $\text{Im } \phi_{t\chi}$ analogous to H^0 in eq. (3.37), labeled A^0 , has a large mass given by eq. (3.38). The other linear combination is the Nambu-Goldstone boson that becomes the longitudinal Z . At order ϵ , the longitudinal Z includes a mixture of $\text{Im } \phi_{\chi\chi}$ and $\text{Im } \phi_{\chi t}$. The other two CP-odd mass eigenstates, $A_{\chi\chi}^0$ and $A_{\chi t}^0$ are predominantly $\text{Im } \phi_{\chi\chi}$ and $\text{Im } \phi_{\chi t}$, respectively, and have large masses:

$$M_{A_{\chi\chi}^0, A_{\chi t}^0}^2 = \frac{2}{\epsilon^2} m_{t\chi}^2 \left[1 + b^2 + \frac{M_{\chi\chi, \chi t}^2}{-M_{t\chi}^2} (1 - \rho b^2) + \mathcal{O}(\epsilon^2) \right]. \quad (3.41)$$

These two neutral mass eigenstates are the pseudo Nambu-Goldstone bosons discussed in ref. [3], and are light provided $M_{\chi\chi}^2$ and $M_{\chi t}^2$ are close to their bound (3.15).

The composite scalar spectrum has several features which warrant further comments. The typical scale for the masses of the physical states corresponding to the two weak-doublets and two weak singlets which acquire VEVs is given by $m_{\chi\chi} = m_{t\chi}/\epsilon$. By contrast, the h^0 has a mass proportional to $m_{t\chi}$, so that is a light state in the limit $\epsilon \rightarrow 0$. The reason for this result is the fact that the unitarity of the WW scattering cross-section requires a state of the order of the electroweak scale, and the electroweak symmetry breaking VEVs, $v_{t\chi}$ and v_{tt} , are suppressed by a factor of ϵ compared with the other VEVs. Therefore, the upper bound on the standard model Higgs boson mass, of order 1 TeV [6], is automatically enforced within our composite Higgs sector.

The further suppression which allows $M_{h^0} \ll 1$ TeV when $M_{\chi\chi}^2 \approx M_{t\chi}^2$ is of a different nature. To see this, one should recall that, to leading order in b^2 , $C_{\chi\chi} \rightarrow 0$ (and also $\mu_{\chi\chi} \rightarrow 0$) when $M_{\chi\chi}^2 \rightarrow M_{t\chi}^2$ [see eq. (3.15)]. In this case, decreasing $M_{\chi\chi}^2$ triggers a second order phase transition from the viable vacuum discussed thus far, to a new minimum of the effective potential where only the weak-singlet fields $\phi_{\chi t}$ and $\phi_{\chi\chi}$ have nonzero VEVs. The h^0 mass is therefore controlled by the proximity of $M_{\chi\chi}^2$ to the critical point. Note that we computed the lightest Higgs boson mass only to leading order in b^2 , so that it is not clear whether the phase transition is truly second order or weakly first order (in which case there is a theoretical lower bound on M_{h^0} , but that may be below the experimental bound of ~ 100 GeV).

It is also easy to understand why both h^0 and $A_{\chi\chi}^0$ have squared-masses proportional to $M_{\chi\chi}^2 - M_{t\chi}^2$ [or equivalently, to $\mu_{\chi\chi}$ as follows from eq. (3.29)] in the limit of small b^2 . When $\mu_{\chi\chi} \rightarrow 0$, $A_{\chi\chi}^0$ becomes the Nambu-Goldstone boson associated with a global $U(1)_\chi$ symmetry broken spontaneously by the $v_{\chi\chi}$ VEV, while the h^0 is the order parameter of a second order phase transition.

To summarize, the composite scalar spectrum consists of the longitudinal W and Z

and the following states:

- h^0 : a neutral Higgs boson of mass $m_{t\chi} \sim 600$ GeV times a factor of order one (or smaller if $M_{\chi\chi}^2 \approx M_{t\chi}^2$);
- H^0, H^\pm, A^0 : the heavy states of a two Higgs-doublet sector, roughly degenerate with a mass $(m_{t\chi}/\epsilon)\sqrt{2/\rho}$;
- $H_{\chi t}^0, A_{\chi t}^0$: one CP-even and one CP-odd state, which are light only if $M_{\chi t}^2 \approx M_{t\chi}^2$;
- $A_{\chi\chi}^0$: a neutral CP-odd state which is light only if $M_{\chi\chi}^2 \approx M_{t\chi}^2$.
- ϕ_{bb} : a neutral complex scalar, with a mass M_{tb} (which is an arbitrary parameter);
- H_{tb}^\pm : a charged scalar which can be as light as 250 GeV if M_{tb} and $M_{\chi b}$ are sufficiently small;
- $H_{\chi\chi}^0, H_{\chi b}^\pm$: a CP-even neutral state and a charged scalar, with large masses, $\gtrsim m_{t\chi}/\epsilon$.

Finally we note that, for a generic choice of parameters, one or more of these scalars may have a mass of order the cutoff, M . If so, these particles are not part of the low-energy effective theory.

4 Higher Energy Physics

We have shown in the previous Section that the top quark seesaw mechanism leads to a low-energy effective theory involving bound states of the χ , t and b quarks. There are several questions that remain: What breaks the topcolor gauge group? What interactions distinguish χ , t and b ? How is electroweak symmetry breaking communicated to the other quarks and leptons? In this Section we describe a class of models of electroweak flavor symmetry breaking incorporating a top quark seesaw which illustrates some of the issues involved in constructing more complete models.

In the prototype model, topcolor symmetry breaking will be dynamically generated while flavor symmetry breaking will be assumed to arise from unspecified “extended topcolor” interactions (analogous to extended technicolor interactions [12]) at higher energies. The model is most easily displayed in “moose notation” [13], in which lines stand for fermion fields and circles for $SU(n)$ gauge groups. An arrow emerging from a circle

with an n in it represents a left-handed fermion transforming like n or a right-handed fermion transforming like \bar{n} , while an arrow going in indicates a right-handed fermion transforming like n or a left-handed fermion transforming like \bar{n} .

Using this notation, the prototype model is shown in Fig. 1. The $\chi_{L,R}$ fields and

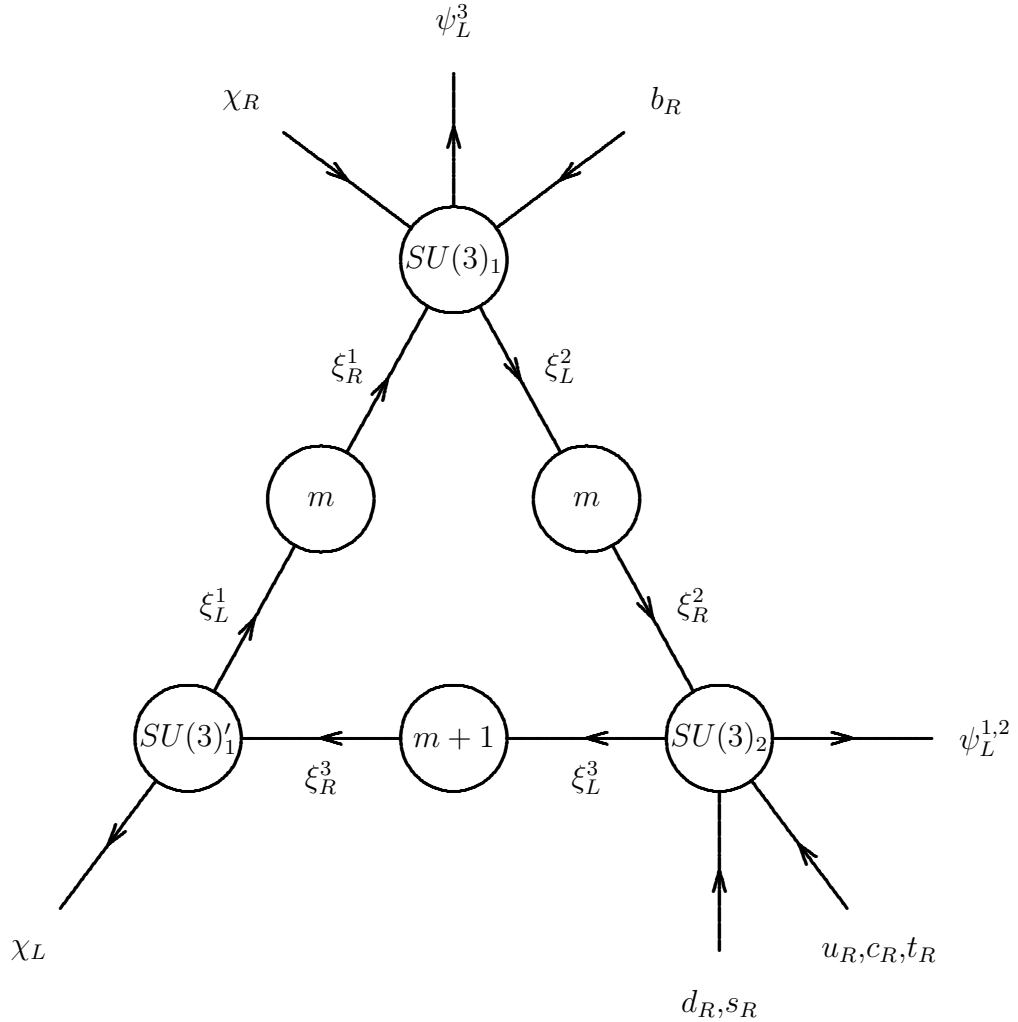


Figure 1: The “moose” model of dynamical topcolor symmetry breaking.

right-handed quark fields are shown explicitly, while $\psi_L^{1,2,3}$ denote the three generations left-handed weak-doublet quark fields. We will assume here that the two $SU(m)$ interactions and the $SU(m+1)$ interactions become strong and produce $\bar{\xi}\xi$ condensates. The (relatively) strong $SU(3)_1$ interactions and the weaker $SU(3)_2$ gauge group are as in the schematic model of Section 2: $SU(3)_1 \times SU(3)'_1 \times SU(3)_2 \rightarrow SU(3)_{QCD}$ due to the formation of $\bar{\xi}_R^1 \xi_L^1$ and $\bar{\xi}_R^2 \xi_L^2$ condensates driven by a strong $SU(m)$ gauge interactions, and a $\bar{\xi}_R^3 \xi_L^3$ condensate driven by a strong $SU(m+1)$ gauge interaction.

The scale of $SU(3)_1 \times SU(3)'_1$ breaking (set by the $\bar{\xi}_L \xi_R$ condensates, *i.e.* the scales at which the two $SU(m)$ interactions and the $SU(m+1)$ interaction become strong) is assumed to be close to the scale at which the $SU(3)_1$ interactions would break the chiral symmetries associated with the χ_R and ψ_L^3 fields. If that chiral phase transition is second-order, this breaking gives rise to a $\bar{\chi}_R \psi_L^3$ composite Higgs field.

The $\mu_{\chi\chi}$ and $\mu_{\chi t}$ “mass” terms cannot be present at tree-level since the corresponding mass operators are not gauge-invariant. Instead, they must arise from higher-dimensional operators coming from higher-energy interactions. A $\bar{\chi}_L \chi_R$ mass term can arise from an operator of the form

$$\bar{\chi}_L \gamma^\mu \xi_L^1 \bar{\xi}_R^1 \gamma_\mu \chi_R, \quad (4.1)$$

giving

$$\mu_{\chi\chi} \propto \langle \bar{\xi}_R^1 \xi_L^1 \rangle, \quad (4.2)$$

while a $\bar{\chi}_L t_R$ mass term can arise from a four-fermion operator of the form

$$\bar{\chi}_L \xi_R^3 \bar{\xi}_L^3 t_R, \quad (4.3)$$

giving

$$\mu_{\chi t} \propto \langle \bar{\xi}_R^3 \xi_L^3 \rangle. \quad (4.4)$$

As these “masses” are proportional to different condensates, their sizes can naturally be different even if the sizes and strengths of the corresponding higher-energy interactions are similar. Furthermore, operators of the form shown in eq. (4.3) can involve all three generations of charge 2/3’s quarks and is a potential source of mixing between the third generation and the first two.

A crucial feature of the seesaw mechanism is that the $\bar{\psi}_L t_R$ mass term must be suppressed. This happens naturally in the model shown in Fig. 1: no gauge-invariant four-fermion operator exists which could give rise to such a term. The largest contributions come from six-fermion operators and are naturally small.

The masses and mixings of the first two generations can easily arise from higher-energy interactions as well, since both the left-handed and right-handed quarks transform under the $SU(3)_2$ interactions. For example, a charm-quark mass can arise from an operator of the form

$$\bar{\psi}_L^3 \chi_R \bar{c}_R \psi_L^2. \quad (4.5)$$

The b mass, however, is quite different here than in the schematic model. Because of the presence of the ξ_R^1 and ξ_L^2 fields which also transform under $SU(3)_1$, instanton

effects yield high-dimension multifermion operators which are too small to account for the bottom-quark mass. We believe this will remain true in any model of dynamical topcolor symmetry breaking. Thus we have assumed, counter-intuitively, that the b_R shares topcolor interactions with ψ_L^3 and χ_R so that we can allow for the operator

$$\epsilon^{\alpha\beta} \overline{\psi_{L\alpha}^3} \chi_R \overline{\psi_{L\beta}^3} b_R \quad (4.6)$$

(the $\epsilon^{\alpha\beta}$ acts on the $SU(2)_W$ indices to make it a singlet). In addition to a b -quark mass, this operator induces a tadpole term for ϕ_{bb} in the effective potential. However, the shift in the vacuum is small if M_{tb} is large, and the analysis in Section 3 remains essentially unaltered.

Having given the χ_R and the b_R the same strong gauge interaction quantum numbers, we must introduce additional interactions to “tilt” the vacuum and prevent the formation of a potentially large $\overline{b_R} \psi_L^3$ condensate and a large bottom-quark mass. In the spirit of extended technicolor, we will assume that the effective Lagrangian includes operators like

$$\frac{\eta_\chi}{M^2} \overline{\psi_L^3} \chi_R \overline{\chi_R} \psi_L^3 + \frac{\eta_b}{M^2} \overline{\psi_L^3} b_R \overline{b_R} \psi_L^3, \quad (4.7)$$

with $\eta_\chi > \eta_b$. Such a pattern of interactions can tilt the vacuum, as required. The presence of the operators in eq. (4.7) give rise to contributions to the T parameter [9], beyond those in eq. (3.25) coming from fermion loops. However, due to the large scale $M \sim \mathcal{O}(50 \text{ TeV})$, these contributions are negligible [3]. The same argument applies in the case of other electroweak observables [14] or FCNC effects [15].

While we have yet to complete a full phenomenological analysis of this model, we regard it as an existence proof that it is possible to construct a model incorporating a top quark seesaw mechanism in which topcolor symmetry breaking is dynamical and which allows for intergenerational mixing. This model also raises additional questions: What gives rise to the necessary higher-energy interactions? Is there a natural explanation for the near equality of the chiral symmetry breaking scales of the $SU(m)$ and $SU(m+1)$ interactions? Why are these chiral symmetry breaking scales close to the scale of $SU(3)_1$ chiral symmetry breaking?

Finally, we note that a variant of this model could be constructed by replacing the b_R fermions transforming under $SU(3)_1$ by the ω_R fermions of eq. (2.26), adding the b_R to the fields transforming under $SU(3)_2$, and adding the ω_L to the fields transforming under $SU(3)'_1$. Anomaly cancellation will then also require that $SU(m+1)$ is replaced by $SU(m+2)$. Such a variant allows for additional sources of mixing between the third generation and the first two.

5 Conclusions

In the dynamical top quark seesaw mechanism EWSB occurs via the condensation of the left-handed top quark with a new, right-handed weak-singlet quark. The fermionic mass scale of this weak $I = 1/2$ condensate is large, of order 0.6 TeV, and it corresponds to the formation of a dynamical boundstate Higgs scalar with a VEV $v/\sqrt{2} \approx 175$ GeV. However, the new χ -quarks also condense amongst themselves at still larger scales, and have condensates with the right-handed top quark as well. Upon diagonalization of the fermionic mass matrix, the physical top quark mass is suppressed compared to the 0.6 TeV matrix element by a seesaw mechanism. As a result, this class of models allows for a dynamical origin of EWSB and can accommodate a heavy top quark without introducing extra fermions carrying weak-isospin quantum numbers.

In this paper we presented a schematic model with a minimal version of the seesaw which illustrates the essential features of the dynamics. We also presented a calculation of the effective potential in a generic low energy theory that incorporates the dynamical top quark seesaw mechanism. This effective potential allows one to understand the range of parameters required for the seesaw mechanism to be successful. Furthermore, we have computed the spectrum of composite scalars, which includes a potentially light Higgs boson. Finally, we presented class of models of electroweak symmetry breaking which incorporate the top quark seesaw mechanism and in which topcolor symmetry breaking is dynamically generated.

Many issues remain to be explored. Among these are: What is the most elegant method to incorporate the first two generations of quarks and intergenerational mixing, as well as leptons? Is there a natural mechanism for topcolor to break close to its chiral symmetry breaking scale? Are there generic experimental signatures of the top quark seesaw? We believe that the top quark seesaw opens up a wide range of directions in model building which may allow these questions to be answered.

Acknowledgments

We are grateful to Bill Bardeen for stimulating discussions regarding the schematic version of the seesaw and the existence of a light composite Higgs boson. We would like to thank Gustavo Burdman, Nick Evans, Deog Ki Hong, Paul Mackenzie and Elizabeth Simmons for useful conversations. We also thank the Aspen Center for Physics for its hospitality during early stages of this work.

Appendix A: The $U(1)$ Tilting Model

We apply here the effective theory approach discussed in Section 3 to the original model with a dynamical seesaw mechanism [3]. The transformation properties of the third generation fermions under the gauge group are shown in Table 1. The breaking of the gauge group down to the standard model one leaves a degenerate octet of massive ‘‘colorons’’ and two heavy $U(1)$ gauge bosons. It is assumed that all these gauge bosons have a mass $M \sim \mathcal{O}(50 \text{ TeV})$.

The coefficients of the four-fermion operators are given by

$$z_{AB} = \frac{2}{\pi} \left(\frac{N_c^2 - 1}{2N_c} \kappa + Y_A Y_B \kappa_1 + X_A X_B \kappa_{B-L} \right), \quad (\text{A.1})$$

where Y are the $U(1)_1$ charges while X are the $U(1)_{B-L}$ charges, shown in Table 1, and $\kappa, \kappa_1, \kappa_{B-L}$ are the $SU(3)_1 \times U(1)_1 \times U(1)_{B-L}$ coupling constants, defined as the gauge couplings squared divided by 8π .

	$SU(3)_1$	$SU(3)_2$	$SU(2)_W$	$U(1)_1$	$U(1)_2$	$U(1)_{B-L}$
ψ_L	3	1	2	1/3	0	1/3
t_R	3	1	1	4/3	0	$-1/3 < x < 0$
b_R	3	1	1	-2/3	0	1/3
l_L	1	1	2	-1	0	-1
τ_R	1	1	1	-2	0	-1
ν_R^τ	1	1	1	0	0	-1
χ_L	3	1	1	4/3	0	$-1/3 < x < 0$
χ_R	3	1	1	4/3	0	1/3

Table 1: Third-generation and χ fermion representations

The charge assignment implies $M_{\chi t}^2 < M_{\chi\chi}^2 < M_{tt}^2 < M_{\chi b}^2$ and $M_{t\chi}^2 < M_{tb}^2 < M_{\chi b}^2$. The scalars having b_R as constituent do not acquire VEVs provided $M_{tb}^2 > 0$, which gives:

$$-2\kappa_1 + \kappa_{B-L} < 12 \left(\frac{3\pi}{8} - \kappa \right). \quad (\text{A.2})$$

The vacuum alignment condition $M_{t\chi}^2 < 0 < M_{tt}^2$ requires

$$4\kappa_1 + 3x\kappa_{B-L} < 12 \left(\frac{3\pi}{8} - \kappa \right) < 4\kappa_1 + \kappa_{B-L}. \quad (\text{A.3})$$

Finally, the restriction $M_{\chi t}^2 \gtrsim M_{t\chi}^2$ imposed by the minimization condition (3.15) gives

$$12\kappa_1 \lesssim (1 - 9x^2) \kappa_{B-L} . \quad (\text{A.4})$$

The range of the $U(1)_{B-L}$ charge of t_R and χ_L , $-1/3 < x < 0$, allows the conditions (A.2), (A.3) and (A.4) to be simultaneously satisfied.

The relation between the coefficients of the four-fermion operators and the fermion charges leads to relations among the six M_{AB}^2 parameters from the effective potential. These relations are simplified by observing that the non-Abelian coupling constant κ is assumed to be larger than the $U(1)$ coupling constants, which implies the criticality condition:

$$\kappa = \frac{3\pi}{8} + \mathcal{O}(\kappa_1, \kappa_{B-L}) . \quad (\text{A.5})$$

To first order in κ_1/κ and κ_{B-L}/κ one can write down three sum rules:

$$\begin{aligned} M_{tt}^2 - M_{\chi\chi}^2 &\approx M_{\chi b}^2 - M_{tt}^2 \approx 2(M_{tb}^2 - M_{t\chi}^2) \\ M_{\chi\chi}^2 - M_{\chi t}^2 &\approx -3x(M_{tt}^2 - M_{t\chi}^2) . \end{aligned} \quad (\text{A.6})$$

A consequence of the second sum rule is $M_{\chi b} > |M_{t\chi}|$, so that the H_{tb}^\pm charged scalar discussed in Section 3.4 is heavier than $m_{t\chi}/\epsilon$. Therefore, in addition to h^0 , the only composite scalars that may be lighter than $m_{t\chi}/\epsilon$ are the neutral states $A_{\chi\chi}^0$, $A_{\chi t}^0$, $H_{\chi t}^0$, and ϕ_{bb} .

The composite scalar spectrum is a function of the following parameters: κ , κ_1 , κ_{B-L} , x , ϵ and $\ln(M/m_\chi)$. For example, the lightest Higgs boson has a mass:

$$M_{h^0}^2 = 4m_{t\chi}^2 \frac{(1 - 3x)\kappa_{B-L} - 12\kappa_1}{9\pi [1 - 3\pi/(8\kappa)] + 3(1 - x)\kappa_{B-L} - 4\kappa_1} [1 + \mathcal{O}(\kappa_1, \kappa_{B-L}, b^2, \epsilon^2)] . \quad (\text{A.7})$$

In this model, the Higgs boson would have a mass of order 100 GeV only if the ratio κ_1/κ_{B-L} is smaller than $(1 - 3x)/12$ by no more than a few percent.

Appendix B: Equivalence between the Gap Equations and the Stationarity Conditions for the Effective Potential

In this Appendix we show that the set of coupled gap equations used in ref. [3] is identical [in the large N_c limit and for large $\ln(M^2/\overline{M}^2)$] with the stationarity conditions for the effective potential (see Section 3.2).

The four-fermion operators discussed in Section 3 [see eqs. (3.1) and (3.9)] lead to a dynamical mass matrix for the t and χ quarks, given in the weak eigenstate basis by

$$\mathcal{L} = -(\bar{t}_L, \bar{\chi}_L) \begin{pmatrix} m_{tt} & m_{t\chi} \\ m_{\chi t} & m_{\chi\chi} \end{pmatrix} \begin{pmatrix} t_R \\ \chi_R \end{pmatrix} + \text{h.c.}, \quad (\text{B.1})$$

with all the elements real (this can be ensured by a phase redefinition of the fields). The top and χ masses are the eigenvalues of this matrix,

$$m_{t,\chi}^2 = \frac{1}{2} \left[m_{\chi\chi}^2 + m_{tt}^2 + m_{\chi t}^2 + m_{t\chi}^2 \mp \sqrt{(m_{\chi\chi}^2 + m_{tt}^2 + m_{\chi t}^2 + m_{t\chi}^2)^2 - 4(m_{\chi\chi}m_{tt} - m_{t\chi}m_{\chi t})^2} \right] \quad (\text{B.2})$$

while the mass eigenstates are given by

$$\begin{pmatrix} t'_L \\ \chi'_L \end{pmatrix} = \begin{pmatrix} c_L & -s_L \\ s_L & c_L \end{pmatrix} \begin{pmatrix} t_L \\ \chi_L \end{pmatrix},$$

$$\begin{pmatrix} t'_R \\ \chi'_R \end{pmatrix} = \begin{pmatrix} c_R & s_R \\ -s_R & c_R \end{pmatrix} \begin{pmatrix} -t_R \\ \chi_R \end{pmatrix}, \quad (\text{B.3})$$

where

$$c_L, s_L = \frac{1}{\sqrt{2}} \left[1 \pm \frac{m_{\chi\chi}^2 - m_{tt}^2 + m_{\chi t}^2 - m_{t\chi}^2}{m_\chi^2 - m_t^2} \right]^{1/2}, \quad (\text{B.4})$$

and c_R, s_R are obtained by substituting $m_{t\chi} \leftrightarrow m_{\chi t}$ in the above expressions for c_L, s_L .

The one-loop gap equations can be easily computed by keeping the weak eigenstates in the external lines, and the χ and t mass eigenstates running in the loop (see Fig. 2), and are given by:

$$m_{tt} = z_{tt} \left\{ -c_L c_R m_t \left[1 - \frac{m_t^2}{M^2} \ln \left(\frac{M^2}{m_t^2} \right) \right] + s_L s_R m_\chi \left[1 - \frac{m_\chi^2}{M^2} \ln \left(\frac{M^2}{m_\chi^2} \right) \right] \right\}$$

$$m_{\chi\chi} = \mu_{\chi\chi} + z_{\chi\chi} \left\{ -s_L s_R m_t \left[1 - \frac{m_t^2}{M^2} \ln \left(\frac{M^2}{m_t^2} \right) \right] + c_L c_R m_\chi \left[1 - \frac{m_\chi^2}{M^2} \ln \left(\frac{M^2}{m_\chi^2} \right) \right] \right\}$$

$$m_{t\chi} = z_{t\chi} \left\{ c_L s_R m_t \left[1 - \frac{m_t^2}{M^2} \ln \left(\frac{M^2}{m_t^2} \right) \right] + s_L c_R m_\chi \left[1 - \frac{m_\chi^2}{M^2} \ln \left(\frac{M^2}{m_\chi^2} \right) \right] \right\}$$

$$m_{\chi t} = \mu_{\chi t} + z_{\chi t} \left\{ s_L c_R m_t \left[1 - \frac{m_t^2}{M^2} \ln \left(\frac{M^2}{m_t^2} \right) \right] + c_L s_R m_\chi \left[1 - \frac{m_\chi^2}{M^2} \ln \left(\frac{M^2}{m_\chi^2} \right) \right] \right\} \quad (\text{B.5})$$

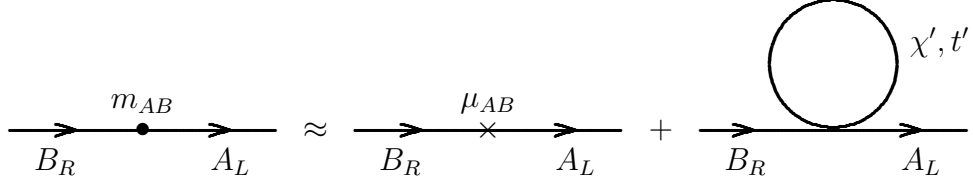


Figure 2: Coupled gap equations ($A, B = t, \chi$).

Using the relation between the mass matrices in the two basis, namely

$$\begin{pmatrix} m_{tt} & m_{t\chi} \\ m_{\chi t} & m_{\chi\chi} \end{pmatrix} = \begin{pmatrix} -c_{LCR}m_t + s_{LSR}m_\chi & c_{LSR}m_t + s_{LCR}m_\chi \\ s_{LCR}m_t + c_{LSR}m_\chi & -s_{LSR}m_t + c_{LCR}m_\chi \end{pmatrix}, \quad (\text{B.6})$$

we can rewrite the gap equations as

$$\begin{aligned} m_{tt}M^2 \left(\frac{1}{z_{tt}} - 1 \right) &= - \left[m_{tt} (m_{tt}^2 + m_{t\chi}^2 + m_{\chi t}^2) + m_{t\chi}m_{\chi t}m_{\chi\chi} \right] \ln \left(\frac{M^2}{m_\chi^2} \right) \\ m_{\chi\chi}M^2 \left(\frac{1}{z_{\chi\chi}} - 1 \right) - \mu_{\chi\chi}M^2 \frac{1}{z_{\chi\chi}} &= - \left[m_{\chi\chi} (m_{t\chi}^2 + m_{\chi t}^2 + m_{\chi\chi}^2) + m_{tt}m_{t\chi}m_{\chi t} \right] \ln \left(\frac{M^2}{m_\chi^2} \right) \\ m_{t\chi}M^2 \left(\frac{1}{z_{t\chi}} - 1 \right) &= - \left[m_{t\chi} (m_{tt}^2 + m_{t\chi}^2 + m_{\chi\chi}^2) + m_{tt}m_{\chi t}m_{\chi\chi} \right] \ln \left(\frac{M^2}{m_\chi^2} \right) \\ m_{\chi t}M^2 \left(\frac{1}{z_{\chi t}} - 1 \right) - \mu_{\chi t}M^2 \frac{1}{z_{\chi t}} &= - \left[m_{t\chi} (m_{tt}^2 + m_{\chi t}^2 + m_{\chi\chi}^2) + m_{tt}m_{t\chi}m_{\chi\chi} \right] \ln \left(\frac{M^2}{m_\chi^2} \right) \end{aligned} \quad (\text{B.7})$$

where we neglected $m_t^3 \ln(m_\chi^2/m_t^2)$ compared with $m_{t,\chi}^3 \ln(M^2/m_\chi^2)$, which is consistent with the leading log approximation used in eqs. (B.5).

One can see that the gap equations (B.7) are identical with the stationarity conditions (3.14) for the effective potential derived in Section 3.

References

- [1] W.A. Bardeen, C.T. Hill and M. Lindner, Phys. Rev. **D 41** (1990) 1647.
- [2] Y. Nambu, report EFI 88-39 (July 1988), published in the Proceedings of the *Kazimierz 1988 Conference on New theories in physics*, ed. T. Eguchi and K. Nishijima; in the Proceedings of the *1988 International Workshop on New Trends in Strong Coupling Gauge Theories*, Nagoya, Japan, ed. Bando, Muta and Yamawaki (World

- Scientific, 1989); report EFI-89-08 (1989); V. A. Miransky, M. Tanabashi and K. Yamawaki, Mod. Phys. Lett. **A4** (1989) 1043; Phys. Lett. **B 221** (1989) 177; W. J. Marciano, Phys. Rev. Lett. **62** (1989) 2793.
- [3] B. A. Dobrescu and C. T. Hill, Phys. Rev. Lett. **81** (1998) 2634, hep-ph/9712319.
- [4] C. T. Hill, Phys. Lett. **B 266** (1991) 419.
- [5] C. T. Hill, Phys. Lett. **B 345** (1995) 483.
- [6] B. W. Lee, C. Quigg, H. Thacker, Phys. Rev. **D16** (1977) 1519.
- [7] T. Appelquist, J. Terning, L. C. R. Wijewardhana, Phys. Rev. **D44** (1991) 877.
- [8] R. S. Chivukula and H. Georgi, BUHEP-98-12 (May 1998), hep-ph/9805478.
- [9] R. S. Chivukula, B. A. Dobrescu and J. Terning, Phys. Lett. **B 353** (1995) 289, hep-ph/9503203.
- [10] Y. Nambu and G. Jona-Lasinio, Phys. Rev. **122** (1961) 345.
- [11] S. Coleman and E. Weinberg, Phys. Rev. **D7** (1973) 1888.
- [12] E. Eichten and K. Lane, Phys. Lett. **B90** (1980) 125;
S. Dimopoulos and L. Susskind, Nucl. Phys. **B155** (1979) 237.
- [13] H. Georgi, Nucl. Phys. **B266** (1986) 274.
- [14] R. S. Chivukula and J. Terning, Phys. Lett. **B 385** (1996) 209, hep-ph/9606233.
- [15] D. Kominis, Phys. Lett. **B 358** (1995) 312, hep-ph/9506305; G. Buchalla, G. Burdman, C. T. Hill and D. Kominis, Phys. Rev. **D 53** (1996) 5185, hep-ph/9510376.